Journal of Catalysis **195,** 352–359 (2000)
doi:10.1006/jcat.2000.3001, available online at http://www.idealibrary.com on IDEAL®

The Formation and Reactions of Hydrogen Cyanide under the Conditions of the Selective Catalytic Reduction of NO by Isobutane on Cu-MFI

Irene O. Y. Liu and Noel W. Cant

Department of Chemistry, Macquarie University, NSW 2109, Australia

Received March 23, 2000; revised July 7, 2000; accepted July 19, 2000

The possible involvement of cyanide species in the isobutane/NO/O_2 selective catalytic reduction (SCR) reaction over Cu-MFI has been investigated. The reaction undergoes gradual deactivation at 275°C with the emergence of cyanogen, not HCN, as a significant product. Loss of activity is accompanied by the formation of a deposit which yields HCN when heated in the absence of oxygen. At 300°C HCN itself undergoes nearly complete oxidation to CO_2 and N_2 for some hours when reacted with O_2 over Cu-MFI. However, deactivation then sets in with the emergence of cyanogen as a product, followed by unreacted HCN and then NH_3. A similar sequence of events occurs more rapidly at lower temperatures and is accompanied by the accumulation of carbon- and nitrogen-containing species, especially adsorbed ammonia, which probably arises through hydrolysis of HCN. Addition of NO then leads to a staged recovery in activity as cyanogen production passes through a maximum, while N_2 is produced initially from adsorbed NH_3 by the NH_3-SCR reaction and subsequently from cyanide species. At 270°C HCN is completely converted to CO_2 and N_2 when reacted in NO/O_2 mixtures but at 200°C the major steady-state product is cyanogen with a yield over 70%. The higher reactivity of HCN in the presence of NO/O_2 compared to that in O_2 alone is attributable to the formation of NO_2. Deactivation during the isobutane/NO/O_2 reaction has similarities to that occurring during the HCN/O_2 one since NO_2 is nearly absent during the SCR reaction under partial conversion conditions as a result of its back conversion to NO through reaction with carbonaceous deposits. As a consequence, while HCN formed during SCR reacts further, some is converted only as far as cyanogen. © 2000 Academic Press

Key Words: **hydrogen cyanide; cyanogen; Cu-MFI; hydrocarbon-SCR; NO + isobutane.**

INTRODUCTION

It has now been a decade since Held *et al.* (1) and Iwamoto *et al.* (2) first reported that Cu-MFI was an effective catalyst for the selective catalytic reduction (SCR) of NO by higher hydrocarbons in the presence of excess oxygen. While its stability is inadequate for use on vehicles (3), it remains the laboratory benchmark for performance with higher hydrocarbons. More recently, attention has turned to Fe-MFI which has been reported as being largely immune to deactivation by steam and SO_2 (4, 5) although reproducibility is a problem (6). While details of the reaction mechanism with both catalysts remain a matter of some debate, the basic characteristics appear to be similar for the two systems. Reactive adsorbed nitro/nitrate species are formed after oxidation of NO to NO_2 (7–10). These species attack the hydrocarbon with eventual formation of nitrogen-containing deposits which can give rise to N_2, most effectively by reaction with NO_2 (8). Tests with model compounds show that this is possible for a variety of C,N and C,N,O structures (11–13).

Most studies of the performance of Cu-MFI have used alkenes, especially propene, but the work of Petunchi *et al.* (14) shows that isobutane is even more effective. Complete conversion of NO to N_2 is possible at temperatures below 300°C when using an equimolar hydrocarbon/NO mixture (15). With Fe-MFI, isobutane is more selective than propane, with complete NO conversion reported in the original work (4, 5) and more than 70% with samples made by vapour-phase ion exchange (16).

In recent work we have shown that hydrogen cyanide is a significant product of the isobutane/NO/O_2 reaction over Fe-MFI made by a solid-state ion-exchange method (17). At moderate conversions of isobutane, the concentration of HCN can exceed that of N_2. Hydrogen cyanide is partially eliminated if water is added, probably through hydrolysis to NH_3 and conversion to N_2 by the NH_3-SCR reaction. It disappears entirely when all isobutane is consumed. One possible pathway for HCN formation is a nitroso → oxime → nitrile sequence with the latter (isobutyronitrile) decomposing to give HCN, and also propene, which is available to participate in further SCR.

Hydrogen cyanide, along with isocyanic acid (HNCO), is also a known side product of the reduction of NO by ethene and propene over Cu-MFI (18–20) but the concentrations produced are much lower than those found when using isobutane over Fe-MFI. There are no reports of HCN formation when using isobutane over Cu-MFI and it was not observed in our measurements with such a catalyst under deactivating conditions at 282°C (21).

The aim of the present work was to re-examine the possible involvement of HCN in the isobutane/NO/O_2 system

0021-9517/00 $35.00

over Cu-MFI and to investigate the reaction of HCN itself over the same catalyst. There is currently very little information in the literature on the behaviour of HCN over oxide or zeolite catalysts and, as far as we know, none for hydrocarbon-SCR systems.

EXPERIMENTAL

The Cu-MFI sample was identical to that used previously (21) and made by exchange of Na-MFI (Si/Al = 11.9, Tosoh Inc.) with copper acetate to an exchange level of 80% (3.2 wt% Cu) followed by drying at 110°C and calcination at 500°C. Testing was carried out using 100-mg samples pressed, crushed, and sieved to a particle size of 300 to 600 μm. The samples were pretreated in 10% O_2/He to a temperature of 480°C before each experiment and cooled in helium. The standard test gas (1000 ppm isobutane, 1000 ppm NO, 3% O_2, balance helium to a total flow of 100 cm^3(STP)/min) was made by blending standard gas mixtures using electronic flow meters.

The HCN stream was made by decomposition of formamide. A side stream of helium (10 cm^3/min) was fed through liquid formamide held at 83.5°C giving a partial pressure of ~3600 ppm which was then passed through a Pyrex tube containing Pyrex chips held at 490°C. There was nearly complete decomposition to HCN and water. The latter, together with traces of unreacted formamide, was removed by passage through a Drierite trap at room temperature. The dry HCN/He was then introduced into the main stream in place of part of the helium carrier giving a final HCN concentration of ≈360 ppm.

The gas stream leaving the reactor, or the reactant stream on bypass, was analysed by a combination of FTIR (Mattson Cygnus 100) and micro gas chromatography (MTI Instruments, model M200) as described previously (17, 22) except that the temperature of the Poraplot U column was raised to 120°C. This provided good peak shapes for cyanogen (with retention time of 31 s) and hydrogen cyanide (51 s). Since neither HCN nor C_2N_2 was available as a standard mixture, their peak areas on the micro thermal conductivity detector were converted to concentrations assuming sensitivities equal to those of similar molecules (CO and butadiene, respectively). The assumption should be quite good based on the trends in the tabulations of Dietz (23). The detection limits were less than 5 ppm. Hydrogen cyanide was also analysed by FTIR at 712.1 cm^{-1} as described previously (22) with a detection limit of 10 ppm. The correlation with the GC method was very high (correlation coefficient >0.995) but the FTIR analyses averaged ≈20% higher. Only the FTIR values are given later since that method should be more accurate as it is an absolute one which uses synthetic spectra generated from a high-accuracy data base (24). Nonetheless, the possibility of a modest systematic error should be borne in mind. The infrared bands of cyanogen are much weaker than those of HCN and were not detectable by FTIR. Instead its correct identification was confirmed by on-line mass spectrometry using a Balzers Thermostar quadrupole instrument. The intensities of peaks with m/z of 52 and 26, which are characteristic of cyanogen, followed the same trends as the areas of the corresponding gas chromatographic peaks.

RESULTS

The Isobutane-SCR Reaction

Figure 1 shows the performance of the present Cu-MFI catalyst for the isobutane-SCR reaction as a function of temperature with points obtained in random order allowing ~50 min at each temperature. As reported by Petunchi and Hall (15), the effectiveness for NO removal is very high. Conversion exceeds 95% above 305°C, at which temperature the conversion of isobutane is ~75%. Carbon dioxide is then the sole carbon-containing product but a significant fraction of CO is produced at lower temperatures. Almost all NO is converted to N_2. Hydrogen cyanide was not detectable (<5 ppm) at any temperature. However, cyanogen (C_2N_2) was observed at some temperatures below 300°C if the system was allowed to equilibrate for prolonged periods.

The behaviour for an experiment commenced at 275°C is shown in Fig. 2. Cyanogen starts to emerge after 70 min and stabilises at ~18 ppm. The absence of cyanogen during the initial stages may be due to adsorption since mass balance calculations over that period showed a significant deficit (>10%) in both carbon and nitrogen. It is also noteworthy that although little CO is formed initially, its concentration

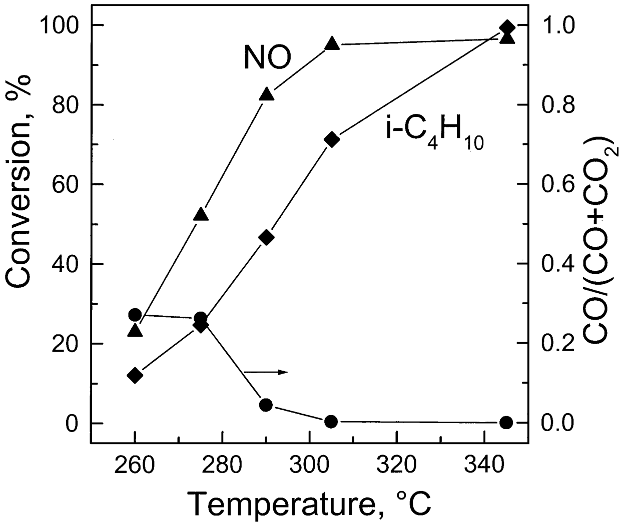

FIG. 1. Conversions and $CO/(CO + CO_2)$ ratio as a function of temperature during the reaction of 1000 ppm isobutane with 1000 ppm NO and 3% O_2 over 100 mg of Cu-MFI with GHSV ≈ 30,000 h^{-1}.

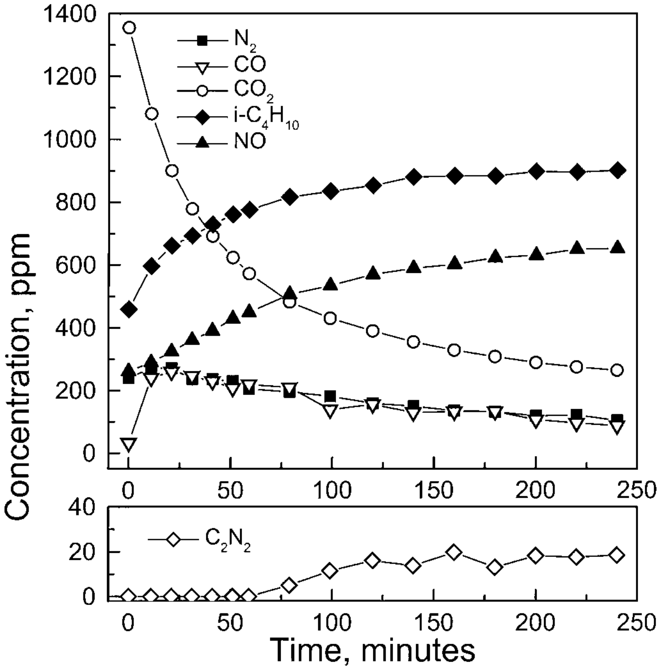

FIG. 2. Concentrations as a function of time during the reaction of 1000 ppm isobutane with 1000 ppm NO and 3% O_2 over 100 mg of Cu-MFI at 275°C with GHSV ≈ 30,000 h^{-1}.

rises to a maximum after 20 min, and that it comprises ~30% of the carbon-containing products once cyanogen production stabilises. In similar tests at temperatures of 310°C and above, conversions of NO were nearly complete initially and deactivation was not observable even over periods of many hours. Cyanogen was never detectable and the CO/CO_2 ratio was below 0.01 throughout. The only previous reports of cyanogen formation in hydrocarbon-SCR systems have been for trace amounts in trapped products when using propene over Cu-MFI (25) and propane over Fe-MFI (26). Larger amounts have been observed during the reaction of NO_2/O_2/propene mixtures over sodium zeolites including Na-MFI (27).

The product distribution between substances that evolved when the partially deactivated Cu-MFI sample from the above experiment was ramped to 470°C in helium alone is shown in Fig. 3. The first product to appear is carbon dioxide with peak production at 360°C followed by carbon monoxide with a maximum at 390°C. However, the substance produced in the largest amount overall is HCN (~105 μmol/g, HCN/Cu ≈ 0.2). Thus, although the isobutane/NO/O_2 reaction itself does not give rise to appreciable HCN under steady-state conditions it does lay down reactive deposits which are capable of generating it on heating. A subsequent temperature-programmed oxidation of the sample in 3% O_2/He starting from 275°C gave only CO_2 and N_2 with peak production at temperatures of 370°C and 330°C, respectively.

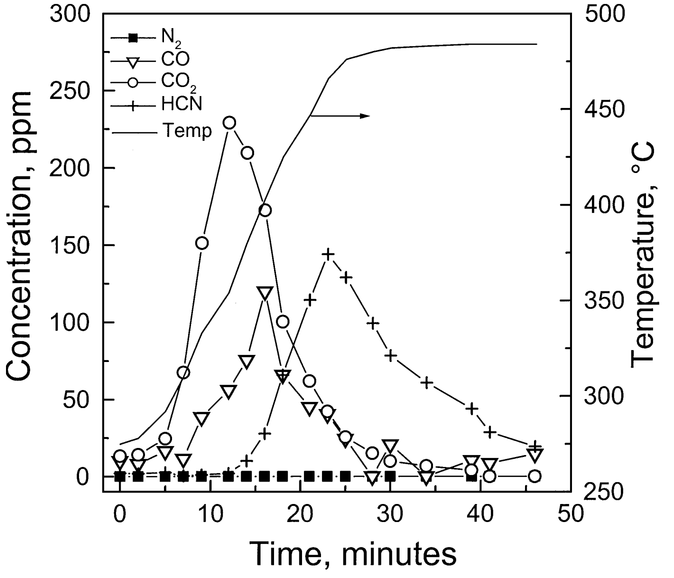

FIG. 3. Product concentrations versus time during the heating of Cu-MFI, deactivated by exposure to a mixture of isobutane, NO, and O_2 for 4 h at 275°C as per Fig. 2, in helium.

The results of a further experiment in which the regenerated Cu-MFI sample was again exposed to isobutane/NO/O_2 for 4 h at 275°C and then exposed to NO_2/He are illustrated in Fig. 4. In this case both CO_2 and N_2 are produced

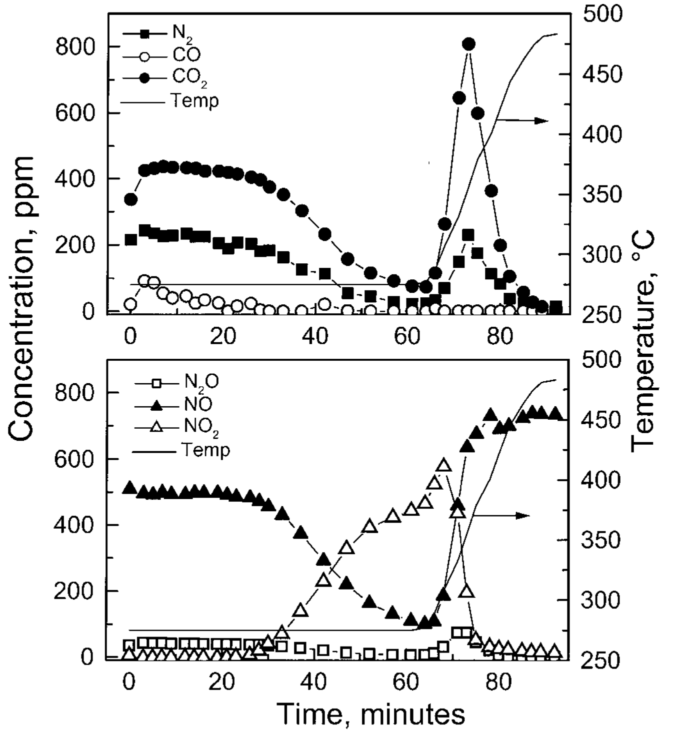

FIG. 4. Product distribution versus time following exposure of Cu-MFI, deactivated by exposure to a mixture of isobutane, NO, and O_2 for 4 h at 275°C as per Fig. 2, to 800 ppm NO_2/He.

immediately in the approximate ratio of 2 : 1. There is no residual NO_2. Approximately one-third ends up as N_2, the rest as NO. This situation continues for ~25 min at 275°C when some unreacted NO_2 commences to emerge. Simultaneously formation of CO_2, N_2, and NO declines in unison until, after 65 min, their values are about one-fifth of the initial plateau values. Ramping the temperature then gives a slight increase in NO_2 concentration followed by a second simultaneous production of CO_2 and N_2, also accompanied by extensive conversion of NO_2 to NO. The latter remains dominant after formation of CO_2 and N_2 ceases since the temperature (>450°C) is then such that the catalyst is very active for the decomposition of NO_2 to NO and O_2.

Reactions of HCN

The observation of cyanogen rather than HCN in experiments such as that illustrated by Fig. 2 could be a consequence of the high reactivity of HCN under SCR conditions. Initial tests of this possibility were carried out using HCN in O_2/He alone. Figure 5 shows the behaviour at 300°C. Carbon dioxide and nitrogen are the sole products for the initial 200 min but the amount of N_2 produced is less than one-half that of CO_2 as one would anticipate from oxidation alone, i.e.,

$$4HCN + 5O_2 \rightarrow 4CO_2 + 2N_2 + 2H_2O. \qquad [1]$$

This is because the mass balance in nitrogen, and to a very much smaller extent in carbon, is incomplete. Thus species, largely containing nitrogen, are being accumulated. The product distribution changes after 180 min. Formation of CO_2 and N_2 starts to decline steeply and cyanogen appears followed closely by unreacted hydrogen cyanide. Finally, after 300 min, small concentrations of ammonia and carbon monoxide are also observable.

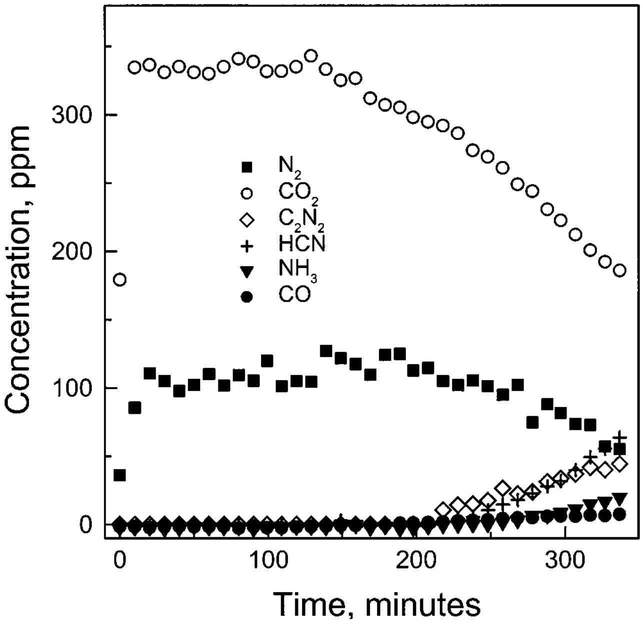

FIG. 5. Concentrations as a function of time during the reaction of 360 ppm HCN with 3% O_2 over 100 mg of Cu-MFI at 300°C with GHSV ≈ 30,000 h^{-1}.

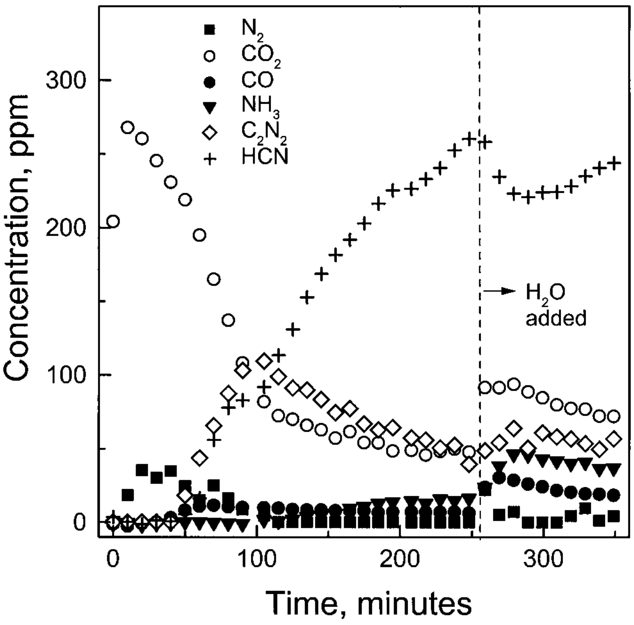

FIG. 6. Concentrations as a function of time during the reaction of 360 ppm HCN with 3% O_2 over 100 mg of Cu-MFI at 260°C with GHSV ≈ 30,000 h^{-1} followed by addition of 1800 ppm H_2O/He.

This sequence of product appearance is seen more clearly at lower temperatures. Figure 6 shows the results of an experiment at 260°C in which the effect of added water was also tested. As at 300°C, all HCN is removed initially but the amount of CO_2 formed corresponds to much less than the carbon in the HCN lost. More strikingly, little N_2 or other nitrogen-containing products are observed. Thus species containing both carbon and nitrogen, especially the latter, are accumulating rapidly. Formation of cyanogen becomes noticeable after 60 min and reaches a maximum of ~100 ppm at 100 min, after which time its concentration exceeds that of CO_2. Unreacted HCN and a small amount of CO break through shortly after cyanogen followed by ammonia which attains a steady concentration of 20 ppm from 200 min on. Addition of water results in a small drop in HCN concentration, with CO_2, CO, and NH_3 as the products, the latter lagging a little as the amount adsorbed on the catalyst increases to match the higher gas-phase concentration. Cyanogen concentration stabilises at ~60 ppm.

Figure 7 shows the results of a similar experiment but with NO, rather than water, added when deactivation of the catalyst was near complete. The use of a slightly higher temperature (270°C rather than 260°C) results in the generation of more N_2 initially but loss of carbon and, especially, nitrogen to the catalyst remains evident. Similarly,

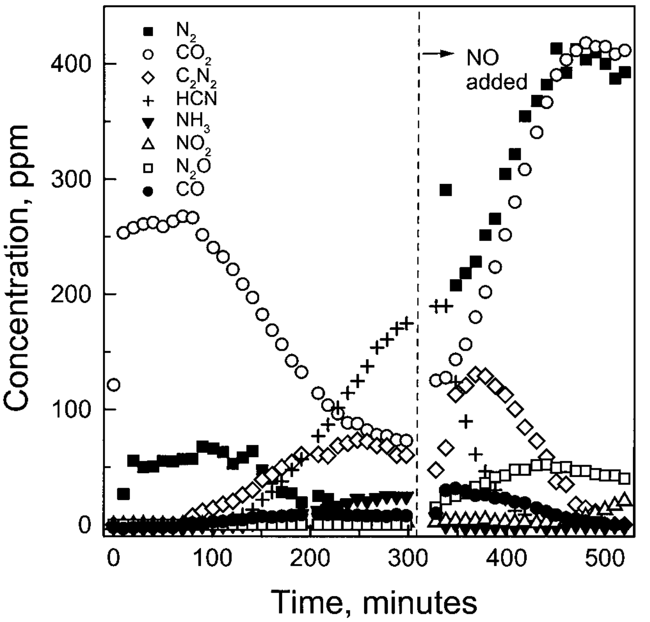

FIG. 7. Concentrations as a function of time during the reaction of 360 ppm HCN with 3% O_2 over 100 mg of Cu-MFI at 270°C with GHSV $\approx$ 30,000 h^{-1} followed by addition of 1000 ppm NO/He.

evolution of cyanogen is delayed somewhat and its peak concentration, as HCN breaks through, is lower than that at 260°C. Again a small but readily measurable amount of NH_3 then becomes evident after a further delay. Introduction of NO produces a dramatic effect. Considerable nitrogen is generated immediately, and all ammonia disappears, but the amount of N_2 formed early on cannot be quantified as only one N_2 analysis is possible during this initial peak. Thereafter the catalyst regains activity, first converting HCN largely to C_2N_2 and some CO, the concentrations of which pass through maxima, but then to CO_2, N_2, and some N_2O. After 200 min of exposure to NO, HCN conversion is complete and the N_2-to-CO_2 ratio approaches unity as expected for the stoichiometry

$$4HCN + 4NO + 3O_2 \rightarrow 4CO_2 + 4N_2 + 2H_2O. \quad [2]$$

At the same time, and notably, a small amount of NO_2 becomes apparent due to NO oxidation.

The behaviour of the HCN/O_2 system over Cu-MFI in the absence and presence of NO at the still lower temperature of 220°C is shown in Fig. 8. The initial stages are quite similar to those at both 260°C (Fig. 6) and 270°C (Fig. 7) except that less CO_2, and no N_2, is formed (i.e., deposition of carbon- and nitrogen-containing species is even more pronounced). Deactivation sets in earlier, accompanied by the emergence of cyanogen, a small amount of CO, and then unreacted HCN as before, but NH_3 is not evident even after 190 min possibly because the adsorption capacity for NH_3 is greater at the lower temperature. Addition of NO results in a large peak in N_2 formation after which the N_2 concentration declines to a steady value equal to that of CO_2. As at 270°C a small amount of N_2O is also generated. However, unlike the behaviour at 270°C (Fig. 7), some HCN and CO remain at near steady state where cyanogen is the dominant product accounting for >60% of the HCN converted.

The results of a further experiment in which HCN and O_2 were reacted with NO present from the beginning at the still lower temperature of 200°C are shown in Fig. 9. Carbon dioxide and nitrogen are now formed in nearly equal amounts from the beginning but the amount of the former accounts for less than 60% of the carbon in the HCN lost. Thus a carbon-containing species is being stored. Almost certainly this species also contains nitrogen but that cannot be assessed accurately from the mass balance because of the large amount of nitrogen present as NO. Cyanogen emerges after 40 min and plateaus at ~150 ppm when it accounts for about two-thirds of the HCN converted. Carbon monoxide is a minor product but there is no ammonia, possibly due to adsorption. When the temperature is subsequently raised to 270°C the product distribution moves rapidly to that in the final stage of the experiment in Fig. 7 (i.e., after NO had been added to a HCN/O_2 feed at the same temperature). There is complete conversion of HCN to CO_2 and N_2 alone apart from some NO_2 produced by oxidation of NO and a lesser amount of N_2O.

The results of tests on the oxidation of CO, NH_3, and NO, alone and in mixtures, at 245°C are shown in Table 1. It is noteworthy that although the conversions of CO and NH_3 are similar when tested alone, their behaviour is very

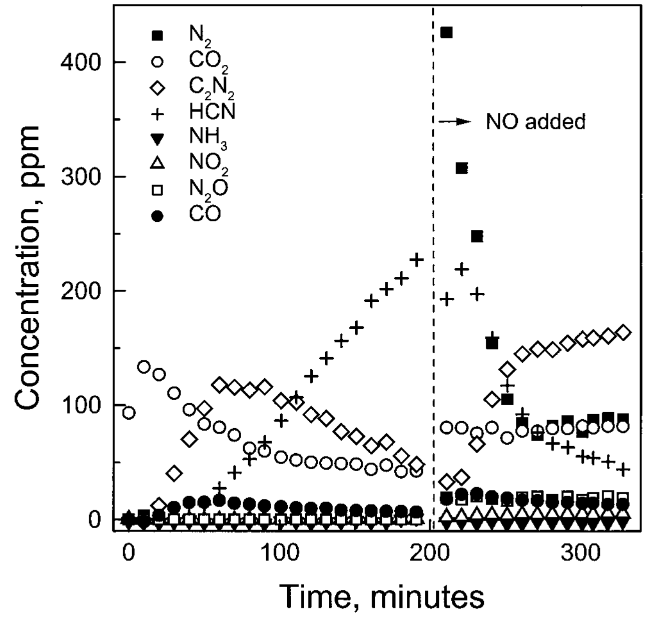

FIG. 8. Concentrations as a function of time during the reaction of 360 ppm HCN with 3% O_2 over 100 mg of Cu-MFI at 220°C with GHSV $\approx$ 30,000 h^{-1} followed by addition of 1000 ppm NO/He.

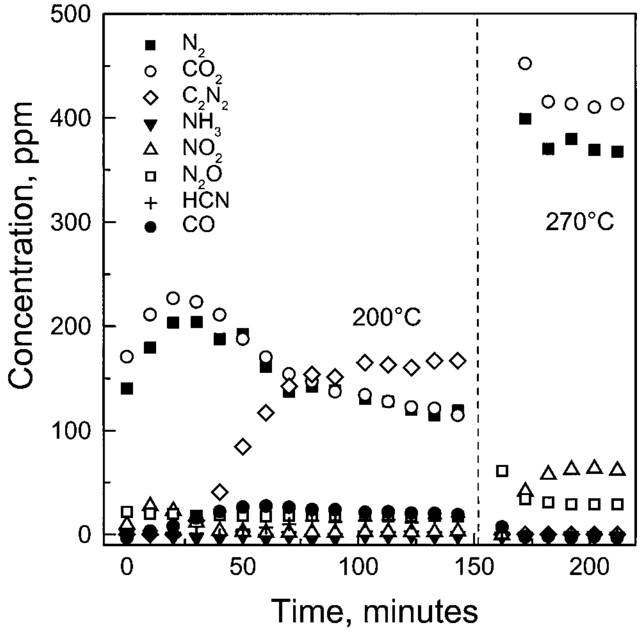

FIG. 9. Concentrations as a function of time during the reaction of 360 ppm HCN with 1000 ppm NO and 3% O_2 over 100 mg of Cu-MFI at 200°C with GHSV ≈ 30,000 h^{-1} followed by heating to 270°C.

different in mixtures. The oxidation of CO is greatly reduced by the presence of ammonia but not vice versa. It is also clear that the NH_3-SCR reaction between NO and NH_3 is much faster than the oxidation of ammonia itself and that the former reaction yields a small but significant amount of N_2O. This may be due to the participation of NO_2 in the SCR reaction since although the oxidation of NO to NO_2 is substantial for NO/O_2 mixtures, no NO_2 is seen when NH_3 is also present. Thus NH_3-SCR using NO_2 is a probable source of the N_2O seen when using $HCN/NO/O_2$ mixtures in the experiments of Figs. 7, 8, and 9. The final row of Table 1 shows results with CO, NH_3, and NO all present at 275°C. The rapid NH_3-SCR reaction removes all ammonia, eliminating inhibition of CO oxidation which proceeds to near completion.

TABLE 1

Reactions of CO, NH_3, and NO with 3% O_2/He Alone and in Mixtures

		Conversions, %			
Feed	*T*, °C	CO	NH_3	NO	N_2O/N_2
$CO + O_2$[a]	245	45	—	—	—
$CO + NH_3 + O_2$[a]	245	5	40	—	<0.01
$NH_3 + O_2$[a]	245	—	40	—	<0.01
$NH_3 + NO + O_2$[a]	245	—	>95	>95	~0.05
$NO + O_2$[a]	245	—	—	~35	—
$CO + NH_3 + NO + O_2$[b]	275	>95	>95	~55	<0.01

[a] With concentrations (when present) of 440 ppm CO, 650 ppm NH_3, and 550 ppm NO in 3% O_2.

[b] With concentrations of 440 ppm CO, 440 ppm NH_3, and 1000 ppm NO in 3% O_2.

DISCUSSION

Reactions of HCN in the Presence of NO and O_2

It is clear from the present work that Cu-MFI is a very active catalyst for the reaction of HCN with a mixture of NO and O_2. As shown by the final stages of Figs. 7 and 9, there is complete conversion to CO_2 and N_2 with a small amount of N_2O at 270°C. Removal remains greater than 80% at 220°C and 200°C (Figs. 8 and 9) but the major product is then cyanogen. The latter is not surprising since HCN is known to adsorb dissociatively on CuO with generation of cyanogen at 50°C (28, 29). Furthermore, the original discovery of cyanogen by Gay-Lussac (30) was through decomposition of AgCN and a standard method of preparation is through the reaction of aqueous KCN and $CuSO_4$ (31). In each case the group I metal is reduced, to the metal in the case of silver but to the cuprous state with copper. Stone and Williams (28, 29) formulate the reaction of HCN with CuO surfaces as

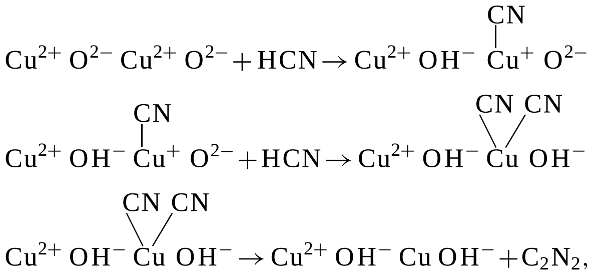

$$\mathrm{Cu^{2+}\,O^{2-}\,Cu^{2+}\,O^{2-} + HCN \rightarrow Cu^{2+}\,OH^{-}\,\overset{CN}{\overset{|}{Cu^{+}}}\,O^{2-}}$$
$$\mathrm{Cu^{2+}\,OH^{-}\,\overset{CN}{\overset{|}{Cu^{+}}}\,O^{2-} + HCN \rightarrow Cu^{2+}\,OH^{-}\,\overset{CN\ CN}{\overset{\backslash /}{Cu}}\,OH^{-}}$$
$$\mathrm{Cu^{2+}\,OH^{-}\,\overset{CN\ CN}{\overset{\backslash /}{Cu}}\,OH^{-} \rightarrow Cu^{2+}\,OH^{-}\,Cu\,OH^{-} + C_2N_2,}$$

i.e., cyanogen formation occurs by pairing of adsorbed cyanide groups and is accompanied by reduction to cuprous hydroxide. A similar process may be feasible on Cu-MFI using extralattice oxygen. At the temperatures used here, decomposition of cuprous hydroxide would yield water while the presence of O_2 and/or NO_x would allow reoxidation to complete the catalytic cycle:

$$\mathrm{Cu^{+}\,OH^{-}\,Cu^{+}\,OH^{-} \rightarrow Cu^{+}\,O^{2-}\,Cu^{+}\,\square + H_2O}$$
$$\mathrm{Cu^{+}\,O^{2-}\,Cu^{+}\,\square + O \rightarrow Cu^{2+}\,O^{2-}\,Cu^{2+}\,O^{2-}}$$

The mechanism by which N_2 rather than C_2N_2 becomes the major product above 220°C is less certain but there appear to be two possibilities. One is the stoichiometrically balanced reaction between adsorbed cyanide and NO_2,

$$\mathrm{CN(ads) + NO_2(ads) \rightarrow N_2 + CO_2.} \qquad [3]$$

This is feasible since the product stream at 270°C, when all HCN is consumed, does contain NO_2 (Figs. 7 and 9). At lower temperatures, where no NO_2 is seen, cyanogen forms (Figs. 8 and 9). Reaction [3] is well established on Co-MFI and Mn-MFI and is believed to be a key step in the selective reduction of NO by methane on those catalysts (32, 33). The second possibility is a two-step process in which HCN is first hydrolysed to ammonia (as seen to some extent in Fig. 6), the ammonia in turn being converted to N_2 by the fast ammonia-SCR reaction (Table 1). Hydrolysis may occur using hydroxyl groups (34) or through hydration to formamide and a standard acid-catalysed process on Brønsted acid sites (35). Recent work in this laboratory has shown that formamide is readily oxidised to N_2 and CO_2 on Cu-MFI at 300°C (36).

Reaction of HCN with O_2 Alone

The behaviour of the HCN/O_2 system is more complex. The conversion is high initially but deactivation sets in so that the eventual conversion at 270°C is less than 50% compared with complete conversion when NO is present (Fig. 7). Deactivation is accompanied by the accumulation of a nitrogen-containing species on the catalyst and the eventual replacement of CO_2 and N_2 as products by cyanogen and ammonia even at 300°C (Fig. 5). A probable explanation for these events is as follows. On initial contact with the oxidised catalyst HCN adsorbs dissociatively to give OH and CN groups as before. Hydroxyl groups may depart as water but the system lacks the NO_2 necessary to remove cyanide by reaction [3]. Removal of cyanide is then limited to the much slower two-step hydrolysis route which generates NH_3 and CO. The former will first be taken up as ammonium ions on Brønsted sites while CO is initially oxidised on unaffected copper sites downstream. However, this sequence is self-limiting. The availability of water at the front of the bed is likely to be insufficient to prevent a progressive build-up of cyanide groups until cyanogen production by pairing becomes possible. Liberation of cyanogen followed by water then reduces the catalyst and depletes the oxide ions needed for dissociation of HCN, which then breaks through.

The changes observed when NO is added to such a deactivated HCN/O_2 system, as in Figs. 7 and 9, are readily explained in terms of the above model. Introduction of NO brings on the fast NH_3-SCR reaction leading to an initial sharp burst of N_2 production as gaseous and adsorbed NH_3 are reacted. Oxidation of NO to NO_2 commences which starts to restore the oxide content, allowing HCN dissociation again. The amount of NO_2 is restricted initially so cyanide groups build up and cyanogen is liberated. As time progresses more NO_2 becomes available. At 270°C this gradually clears cyanide groups by reaction [3] so production of N_2 grows, cyanogen disappears, and NO_2 eventually emerges (Fig. 7). At 220°C the N_2 formation steps are slower, possibly limited by the rate at which NO_2 can be produced, so cyanogen remains a substantial coproduct (Fig. 8).

Cyanide Species in the Isobutane-SCR Reaction

The possible involvement of cyanide species in the isobutane/NO/O_2 reaction, and the deactivation of that reaction at 275°C, can now be examined in the light of the above picture. In the corresponding reaction over Fe-MFI under similar conditions, HCN was observed at concentrations up to 150 ppm (17) but cyanogen was not detectable. With Cu-MFI, by contrast, HCN is below the detection limit here (~5 ppm) but cyanogen reaches 20 ppm (equivalent to 40 ppm HCN). Nonetheless, the data in Figs. 6 to 9 demonstrating that cyanogen is formed readily from HCN over Cu-MFI indicate the involvement of HCN during isobutane-SCR with this catalyst. The probable cause of the difference between the two catalysts is that Fe-MFI is a weaker oxidation catalyst than Cu-MFI as illustrated by the great disparity in CO/CO_2 ratios over the two catalysts: above unity with Fe-MFI at 340°C (16, 17) but less than 0.01 with the present Cu-MFI at the same temperature. If Fe-MFI does not readily abstract hydrogen from HCN, while Cu-MFI does, then if HCN is generated in both systems one expects to see HCN as such with the iron zeolite but cyanogen with the copper one.

The production of cyanogen during isobutane-SCR over Cu-MFI at 275°C (Fig. 2) indicates that the NO_2 concentration is low since C_2N_2 is not observed during the HCN/NO/O_2 reaction at the same temperature when NO_2 is emerging (Figs. 7 and 9). The probable reason for the absence of NO_2 during the isobutane-SCR is obvious. As shown by Fig. 4, it reacts rapidly with material deposited during the reaction and is largely recycled back to NO. This recycling is also well established under steady-state conditions (37).

In our work on isobutane-SCR over Fe-MFI (17) it was postulated that HCN arose as shown in Scheme 1, which involves a nitroso → oxime → nitrile sequence with HCN

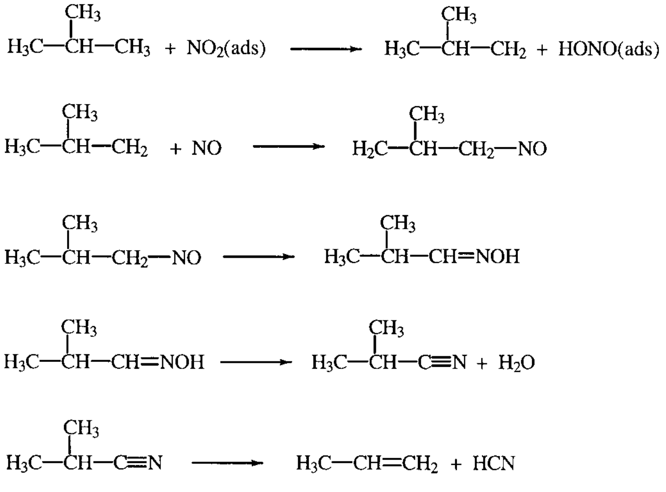

SCHEME 1

formed by elimination from isobutyronitrile. A noteworthy feature of this scheme is that the coproduct to the step generating HCN is propene which is then available to reduce further NO. However, the propene may also undergo polymerisation, probably on Brønsted sites, a process which is thought to be the reason why deposit formation is more pronounced during HC-SCR with propene than with propane (38). The formation of NO when deposits are combusted in NO_2 (Fig. 4) may result from reaction with this purely hydrocarbon material while reduction to N_2 is confined to attack of separate nitrogen-containing species (11–13). In this picture the deposition of carbonaceous material does not have to cause deactivation purely by a site blockage process. Instead, the reactivity of this material towards NO_2 may lower the NO_2 concentration thus allowing other deactivation processes, CN build-up and catalyst reduction, to set in also.

While the above rationalisations can account for the principal observations for the two systems studied here, namely deactivation when using HCN/O_2 but not HCN/NO/O_2 and deactivation with cyanogen formation during the isobutane/NO/O_2 reaction, supporting evidence by way of spectroscopic measurements is highly desirable. However, that was beyond the scope of the study and the capability of the system available.

CONCLUSIONS

Cyanide species appear to play a role in the selective reduction of NO by isobutane over Cu-MFI. Cyanogen is a significant product under partial conversion conditions and the deposits which accumulate during deactivation liberate HCN when heated in the absence of oxidant. Hydrogen cyanide itself is oxidised much more readily by NO/O_2 mixtures than by O_2 alone. Cyanogen can be a significant product of both reactions, being produced during the course of continual deactivation with HCN/O_2 at temperatures below 300°C and in high yields under steady-state conditions at 200°C with HCN/NO/O_2. Complete conversion to CO_2 and N_2 occurs during the latter reaction at 270°C. The much higher reactivity of HCN in the presence of NO can be explained in terms of oxidation of NO to NO_2 which maintains activity through catalyst reoxidation and/or removal of adsorbed cyanide and ammonia. Deactivation during isobutane-SCR at similar temperatures may be facilitated because NO_2 concentrations are kept low through back conversion to NO as a consequence of reaction with carbonaceous deposits.

ACKNOWLEDGMENTS

This work has been supported by grants from the Australian Research Council. We thank Mr. A. Asano of Tosoh Inc. for providing the Na-MFI.

REFERENCES

1. Held, W., König, A., Richte, T., and Puppe, W., Society of Automotive Engineers Technical Paper 900496 (1990).
2. Iwamoto, M., Yahiro, H., Shundo, Y., Yu-U, Y., and Mizumo, N., *Shokubai* **32**, 430 (1990).
3. Matsumoto, S., Yokota, K., Doi, H., Kimura, M., Sekizawa, K., and Kasahara, S., *Catal. Today* **22**, 127 (1994).
4. Feng, X., and Hall, W. K., *Catal. Lett.* **41**, 45 (1996).
5. Feng, X., and Hall, W. K., *J. Catal.* **166**, 368 (1996).
6. Hall, W. K., Feng, X., Dumesic, J., and Watwe, R., *Catal. Lett.* **52**, 13 (1998).
7. Beutel, T., Adelman, B. J., Lei, G.-D., and Sachtler, W. M. H., *Catal. Lett.* **32**, 83 (1995).
8. Chen, H.-Y., Voskoboinikov, T., and Sachtler, W. M. H., *J. Catal.* **180**, 171 (1998).
9. Hadjiivanov, K., Knözinger, H., Tsyntsarski, B., and Dimitrov, L., *Catal. Lett.* **62**, 35 (1999).
10. Lobree, L. J., Hwang, I. C., Reimer, J. A., and Bell, A. T., *Catal. Lett.* **63**, 233 (1999).
11. Beutel, T., Adelman, B., and Sachtler, W. M. H., *Catal. Lett.* **37**, 125 (1996).
12. Iwamoto, M., and Takeda, H., *Catal. Today* **27**, 71 (1996).
13. Chen, H.-Y., Voskoboinikov, T., and Sachtler, W. M. H., *J. Catal.* **186**, 91 (1999).
14. Petunchi, J. O., Sill, G., and Hall, W. K., *Appl. Catal. B* **2**, 303 (1993).
15. Petunchi, J. O., and Hall, W. K., *Appl. Catal. B* **2**, L17 (1993).
16. Chen, H.-Y., and Sachtler, W. M. H., *Catal. Today* **42**, 73 (1998).
17. Liu, I. O. Y., Cant, N. W., Kögel, M., and Turek, T., *Catal. Lett.* **63**, 241 (1999).
18. Radtke, F., Koeppel, R. E., and Baiker, A., *Appl. Catal. A* **107**, L125 (1994).
19. Radtke, F., Koeppel, R. A., and Baiker, A., *Environ. Sci. Technol.* **29**, 2703 (1995).
20. Radtke, F., Koeppel, R. A., and Baiker, A., *Catal. Today* **26**, 159 (1995).
21. Cant, N. W., and Cowan, A. D., *Catal. Today* **35**, 89 (1997).
22. Cowan, A. D., Cant, N. W., Haynes, B. H., and Nelson, P. F., *J. Catal.* **176**, 329 (1998).
23. Dietz, W. A., *J. Gas Chromatogr.* **5**, 68 (1967).
24. Griffith, D. W. T., *Appl. Spectrosc.* **50**, 59 (1996).
25. Gaudin, C., Duprez, D., Mabilon, G., and Prigent, M., *J. Catal.* **160**, 10 (1996).
26. Chen, H.-Y., Voskoboinikov, T., and Sachtler, W. M. H., *Catal. Today* **54**, 483 (1999).
27. Yokoyama, C., and Misono, M., *J. Catal.* **160**, 95 (1996).
28. Stone, F. S., and Williams, T. H., *Stud. Surf. Sci. Catal.* **7**, 1394 (1981).
29. Williams, T. H., Ph.D. thesis, University of Bath, 1975.
30. Gay-Lussac, L. J., *Ann. Chim.* **95**, 172 (1815).
31. Brotherton, T. K., and Lynn, J. W., *Chem. Rev.* **59**, 842 (1959).
32. Lobree, L. J., Aylor, A. W., Reimer, J. A., and Bell, A. T., *J. Catal.* **169**, 188 (1997).
33. Aylor, A. W., Lobree, L. J., Reimer, J. A., and Bell, A. T., *J. Catal.* **170**, 390 (1997).
34. Mellor, J. G., Ph.D. thesis, University of Bristol, 1968.
35. March, J., "Advanced Organic Chemistry," 3rd Edition, p. 338. Wiley, New York, 1985.
36. Cant, N. W., Cowan, A. D., Liu, I. O. Y., and Satsuma, A., *Catal. Today* **54**, 473 (1999).
37. Bethke, K. A., Li, C., Kung, M. C., Yang, B., and Kung, H. H., *Catal. Lett.* **31**, 287 (1995).
38. d'Itri, J. L., and Sachtler, W. M. H., *Appl. Catal. B* **2**, L7 (1993).